

# A deuterated liquid scintillator for supernova neutrino detection

Bhavesh Chauhan <sup>a</sup>, Basudeb Dasgupta <sup>a</sup>,  
and Vivek Datar <sup>b</sup>

<sup>a</sup>Tata Institute of Fundamental Research,  
Homi Bhabha Road, Mumbai 400005, India

<sup>b</sup>Raja Ramanna Fellow, The Institute of Mathematical Sciences,  
CIT Campus, Taramani, Chennai 600113, India

E-mail: [bhavesh@theory.tifr.res.in](mailto:bhavesh@theory.tifr.res.in), [bdasgupta@theory.tifr.res.in](mailto:bdasgupta@theory.tifr.res.in),  
[vivek.datar@gmail.com](mailto:vivek.datar@gmail.com)

**Abstract.** For the next galactic supernova, operational neutrino telescopes will measure the neutrino flux several hours before their optical counterparts. Existing detectors, relying mostly on charged current interactions, are mostly sensitive to  $\bar{\nu}_e$  and to a lesser extent to  $\nu_e$ . In order to measure the flux of other flavors ( $\nu_\mu, \bar{\nu}_\mu, \nu_\tau$ , and  $\bar{\nu}_\tau$ ), we need to observe their neutral current interactions with the detector. Such a measurement is not only crucial for overall normalization of the supernova neutrino flux but also for understanding the intricate neutrino oscillation physics. A deuterium based detector will be sensitive to all neutrino flavors. In this paper, we propose a 1 kton deuterated liquid scintillator (DLS) based detector that will see about 435 neutral current events and 170 (108) charged current  $\nu_e$  ( $\bar{\nu}_e$ ) events from a fiducial supernova at a distance of 10 kpc from Earth. We explore the possibility of extracting spectral information from the neutral current channel  $\bar{\nu}d \rightarrow \bar{\nu}np$  by measuring the quenched kinetic energy of the proton in the final state, where the neutron in the final state is tagged and used to reduce backgrounds.

---

## Contents

<b>1</b>	<b>Introduction</b>	<b>1</b>
<b>2</b>	<b>Methods</b>	<b>5</b>
2.1	Neutrino deuteron interaction cross section	5
2.2	Supernova neutrino fluence and oscillation physics	6
<b>3</b>	<b>Total number of events</b>	<b>8</b>
<b>4</b>	<b>Energy spectrum of events</b>	<b>10</b>
4.1	Neutral current interactions	11
4.1.1	Quenched proton spectrum	11
4.2	Charged current interactions	14
4.2.1	CC interaction of $\nu_e$	15
4.2.2	CC interaction of $\bar{\nu}_e$	15
4.3	Elastic scattering off electrons	16
<b>5</b>	<b>Secondary interactions</b>	<b>16</b>
<b>6</b>	<b>Summary</b>	<b>19</b>
<b>A</b>	<b>Revisiting neutrino deuteron interactions</b>	<b>20</b>
<b>B</b>	<b>Tabulated differential cross sections</b>	<b>23</b>
B.1	$\nu + d \rightarrow \nu + n + p$	23
B.2	$\bar{\nu} + d \rightarrow \bar{\nu} + n + p$	24
B.3	$\nu_e + d \rightarrow e^- + p + p$	25
B.4	$\bar{\nu}_e + d \rightarrow e^+ + n + n$	26
<b>C</b>	<b>Estimating the number of target nuclei <math>N_d</math></b>	<b>27</b>
<b>D</b>	<b>Neutronization Burst</b>	<b>27</b>

---

## 1 Introduction

On average, a supernova occurs every second in our observable universe. The latest theoretical estimates for the rate of core-collapse supernova in Milky Way is approximately 1-2 per 100 years [1, 2]. The last nearby supernova was seen on 23 February 1987 when a  $\sim 20M_\odot$  blue supergiant exploded in the Large Magellanic Cloud approximately 50 kpc away. Neutrino detectors that were operational at the time, e.g., Kamiokande-II [3, 4], IMB [5], and Baksan [6], observed a total of 24 neutrino events, mostly from the electron anti-neutrinos, a few hours before the optical signal. Despite the low statistics, these neutrinos from SN1987 have helped in establishing a baseline

model of supernova explosion and provided a wealth of constraints on new physics scenarios [7–18]. It is now widely held that observation of supernova neutrinos, from the galaxy or even farther away, holds great promise for fundamental physics and astrophysics [19, 20].

Although we now have significantly larger neutrino detectors [21], there remain critical deficiencies in our ability to detect supernova neutrinos. Our best instruments for the purpose, such as Super-Kamiokande [22], LVD [23, 24], HALO [25], and IceCube<sup>1</sup> [27] are mostly sensitive to only the  $\bar{\nu}_e$  flavor, as they depend on the inverse beta decay ( $\bar{\nu}_e + p \rightarrow n + e^+$ ). As a result, the community has set its hopes on future experiments such as DUNE [28, 29], JUNO [30–32], and THEIA [33] to provide sensitivity to  $\nu_e$  and the non-electron flavors, respectively. Hyper-Kamiokande [34] will improve the  $\bar{\nu}_e$  statistics by several orders of magnitude. In this paper, inspired by the success of the previous large-scale deuterium based detector SNO [35], we propose a kton scale deuterated liquid scintillator (DLS) based detector, doped with Gadolinium (Gd), and instrumented with PMTs, which can detect *all the flavors* of supernova neutrinos with spectral information, typically with reduced backgrounds.

The main challenge in deuterium based detectors is the availability of deuterium. India is the one of the world’s largest producers of heavy water, and has the capability to produce a variety of deuterated compounds including deuterated hydrocarbons.<sup>2</sup> It is therefore our understanding that a kton-scale deuterated scintillator detector is realistically achievable. For concreteness, we assume a chemical composition of the form  $C_nD_{2n}$ , mimicking an ordinary scintillator. In practice, significant research is required into identifying a suitable candidate DLS. Much of what we discuss here could also work with a heavy water detector with water soluble ordinary scintillator. We also note that a DLS has previously been used to study neutron capture, albeit with a much smaller detector [36]. To the best of our knowledge, this is the first discussion about using them for neutrino physics.

Neutrino detection in a DLS will be dominantly via dissociation of the deuteron. This proceeds via neutral current (NC) as  $\nu + d \rightarrow \nu + p + n$  or  $\bar{\nu} + d \rightarrow \bar{\nu} + p + n$  for all three flavors, and via charged current (CC) as  $\nu_e + d \rightarrow e^- + p + p$  or  $\bar{\nu}_e + d \rightarrow e^+ + n + n$  for the electron flavor. While the outgoing  $\nu$  or  $\bar{\nu}$  cannot be detected, all the other particles have characteristic signatures. For typical supernova neutrinos with  $E_\nu \sim (5–50)$  MeV, the protons have recoil energies  $\sim (0.1 – 1)$  MeV and are highly non-relativistic. These lead to quenched scintillation signals arising from their high ionization loss  $\sim (10^3 – 10^2)$  MeV cm<sup>-1</sup>. The final state neutrons thermalize due to elastic collisions with the neighboring nuclei and get captured, emitting detectable photons.<sup>3</sup> The final-

---

<sup>1</sup>Even though the primary goal of IceCube is to observe TeV neutrinos, it too can detect supernova neutrinos through the correlated increase in the dark noise rate of its photomultiplier tubes [26].

<sup>2</sup>See for example at <https://www.hwb.gov.in/>

<sup>3</sup>We note that a thermal neutron travels  $\sim 170$  cm in heavy water before capture [37], compared to a few cm in ordinary water [38]. The diffusion length of neutrons in DLS will be much smaller if

**Table 1:** Comparison of final state and detection channels between ordinary detectors and a deuterated scintillator detector. We have not shown some channels that would be common to both, e.g.,  $\nu - e$  and  $\nu - C$  interactions. In the table, *Spectrum* refers to the ability of the detector to reconstruct the incident neutrino spectrum from the channel, whereas *Tagging* refers to having more than one detectable final state particle that can be used to tag signal events against backgrounds.

Flavor	Ordinary Detector		Deuterated Detector	
	Channel	Detector	Channel	Detector
$\bar{\nu}$	$\bar{\nu} p \rightarrow \bar{\nu} p$	JUNO, THEIA <i>Spectrum</i> ✓ <i>Tagging</i> ✗	$\bar{\nu} d \rightarrow \bar{\nu} p n$	SNO <i>Spectrum</i> ✗ <i>Tagging</i> ✗
		HALO <i>Spectrum</i> ✗ <i>Tagging</i> ✗		DLS <i>Spectrum</i> ✓ <i>Tagging</i> ✓
$\nu_e$	$\nu_e \text{Ar} \rightarrow e^- \text{K}^*$	DUNE <i>Spectrum</i> ✓ <i>Tagging</i> ✗	$\nu_e d \rightarrow e^- p p$	SNO <i>Spectrum</i> ✓ <i>Tagging</i> ✗
		HALO <i>Spectrum</i> ✗ <i>Tagging</i> ✗		DLS <i>Spectrum</i> ✓ <i>Tagging</i> ✓
$\bar{\nu}_e$	$\bar{\nu}_e p \rightarrow e^+ n$	SuperK+Gd <i>Spectrum</i> ✓ <i>Tagging</i> ✓	$\bar{\nu}_e d \rightarrow e^+ n n$	SNO <i>Spectrum</i> ✓ <i>Tagging</i> ✓
		LVD, JUNO <i>Spectrum</i> ✓ <i>Tagging</i> ✗		DLS <i>Spectrum</i> ✓ <i>Tagging</i> ✓

state electrons and positrons have energies similar to the incoming neutrinos, thus are highly relativistic, and produce Cherenkov radiation with  $\sim 270$  photons  $\text{cm}^{-1} \text{eV}^{-1}$  [39]. This Cherenkov light arrives earlier than scintillation but is likely to be absorbed and/scattered away by the scintillator.

In Table 1, we give a bird’s eye view comparison of a DLS detector with other prominent neutrino detectors. For the non-electron flavors,  $\nu_\mu, \bar{\nu}_\mu, \nu_\tau,$  and  $\bar{\nu}_\tau,$  NC elastic scattering of a neutrino (or antineutrino) with proton,  $\bar{\nu} p \rightarrow \bar{\nu} p$  [40], can be detected in ordinary scintillator detectors such as JUNO [30–32] and water based scin-

---

*n*-capture dopants, such as Gd, are present. For a more detailed discussion see section 5. The cross sections for neutrons can be obtained from <https://www.nndc.bnl.gov/> or <https://www.ncnr.nist.gov/resources/n-lengths/>.

tillator such as THEIA [33]. With electrons, the relevant cross section is smaller by a ratio  $m_e/E_\nu$ . Although the scintillation signal from the recoil proton is quenched, the one-to-one correspondence between proton kinetic energy and quenched scintillation energy allows for reconstruction of the incident neutrino energy [41]. In contrast, for a DLS, the NC interaction is observed through  $\bar{\nu}d \rightarrow \bar{\nu}np$ . The proton is detected as for an ordinary scintillator. In addition, the final state neutron can be captured. This allows for a possibility to tag the scintillation signal using the associated neutron event and get rid of single-scintillation backgrounds. SNO, a Cherenkov detector, was not sensitive to the low-energy proton recoil and thus had no spectral information on these events. Moving to CC events, ordinarily,  $\bar{\nu}_e$  interacts via inverse beta decay  $\bar{\nu}_e + p \rightarrow e^+ + n$ . The scintillation photons from positron and the delayed photons from the neutron capture provide a clean signal. On the other hand, in a DLS the interaction proceeds through  $\bar{\nu}_e + d \rightarrow e^+ + n + n$ . The additional neutron in the final state doubles the neutron capture efficiency and gives a unique and essentially background-free event signature. Ordinary scintillator detectors can, in principle, observe  $\nu_e$  through its interaction on Carbon. However, due to large threshold and smaller cross section, the sensitivity is expected to be poor [42]. Liquid Argon based detectors like DUNE [28, 29], are hoped to be more sensitive, but significant experimental work remains [43]. Several other ideas have been investigated recently [44–46]. Detecting  $\nu_e$  from a supernova explosion is therefore challenging but important, especially to study the neutronization burst [47]. A DLS is sensitive to  $\nu_e$  through the CC interaction  $\nu_e + d \rightarrow e^- + p + p$ . In comparison with HALO [25], which is a dedicated supernova neutrino detector at SNOLAB, a DLS based detector can be built to be significantly larger. Further, with lead (Pb) as target in HALO, the threshold for neutrino NC and CC interaction is around 10 MeV, whereas for DLS the thresholds are 1.44 (4.03) MeV for  $\nu_e$  ( $\bar{\nu}_e$ ) interacting via CC and 2.22 MeV for NC interactions. Thus, a DLS detector will not only observe larger number of events, but also lower energy neutrinos that cannot be detected by HALO.

Radioactive backgrounds are a crucial concern. If we limit ourselves with backgrounds that could be relevant for galactic supernova neutrino detection, we focus on anything with an event rate that exceeds about 1 per second per kton. In ordinary scintillator detectors the main background comes from the beta decays of  $^{14}\text{C}$  that creates a “wall” of photons at 200 keV and below. For a DLS, photons with energy larger than 2.2 MeV photodissociate the  $d$  in the detector material and pose a potential problem. Beta decays of  $^{208}\text{Tl}$  and  $^{214}\text{Bi}$  in the  $^{238}\text{U}$  and  $^{238}\text{Th}$  chains produce such photons. In SNO great care was taken to reduce this background to about a few hundred per year above 5 MeV. Lower energy photons due to intrinsic and extrinsic radioactivity created a “wall” of photons below 5 MeV. For galactic supernova neutrino detection in DLS, this low energy background could obscure the proton recoil signal. Clearly, one must reduce this background. For NC events the neutrino-induced proton recoil is accompanied by a neutron capture signal. Using the spatial correlation of the neutron capture and proton recoil may help isolate the proton recoil signal away from the background, at least for some fraction of the events. A dedicated study of possible

backgrounds and mitigation techniques is required.

A DLS based detector therefore offers unique advantages, but is not without its challenges. One could detect significant numbers of CC events from both  $\nu_e$  and  $\bar{\nu}_e$  and NC events from all flavors, with spectral information and reduced backgrounds within the same set up. However, in addition to all the usual challenges of building a large scintillator detector with extreme radio-purity, one has the overhead of processing and handling the deuterated chemicals. These challenges, while daunting, are not technologically forbidding. We believe the science-case is promising to motivate further study.

This paper is organized as follows. In Section 2, we discuss the cross sections for neutrino dissociation of deuteron at supernova neutrino energies, and outline our assumptions for supernova neutrino fluxes. In Section 3, we estimate the total number of events seen in 1 kton of DLS for a galactic supernova. As several hundred events are predicted, in Section 4 we explore the possibility to measure the spectrum of events for the four channels. In Section 5, we discuss the interactions of recoiling hadrons which emphasizes the need for adding Gd to the detector. We discuss the avenues for further research and summarize our results in Section 6.

## 2 Methods

### 2.1 Neutrino deuteron interaction cross section

The cross section for neutrino dissociation of deuteron can be calculated in two independent ways. First, using the Phenomenological Lagrangian Approach (PhLA) employed by Nakamura, Sato, Gudkov, and Kubodera (NSGK) [48]. Second, in the framework of Pionless Effective Field Theory ( $\chi$ EFT) valid for  $E_\nu \ll m_\pi$  [49] used by Butler, Chen, and Kong (BCK) [50]. The total cross sections obtained by both methods are in excellent agreement. A discussion about the two approaches can be found in Appendix A. In Figure 1, we see that the total cross sections obtained by NSGK and BCK are very similar up to neutrino energy of 50 MeV. Thus we can safely use  $\chi$ EFT for estimating the supernova neutrino event rates.

For this paper, we have used the tabulated numerical values from NSGK where total cross sections are required. However, for the differential cross sections, NSGK only provides plots for a few energies, whereas BCK provides analytical expressions in terms of the outgoing lepton energy, which is unmeasurable for the NC channel. We therefore recomputed all the differential cross sections in terms of measurable energies, i.e., specifically for the proton in NC channel, using the method of BCK. As a cross check we compared the total cross section obtained from the above to the NSGK results. In doing so, we found anomalies that were traced back to a typo in one of the expressions in BCK.<sup>4</sup> After these corrections, the differential cross sections thus

---

<sup>4</sup>We thank J. W. Chen for sharing with us his original calculations and pointing out the typo in the published version, following which we could reproduce their results.

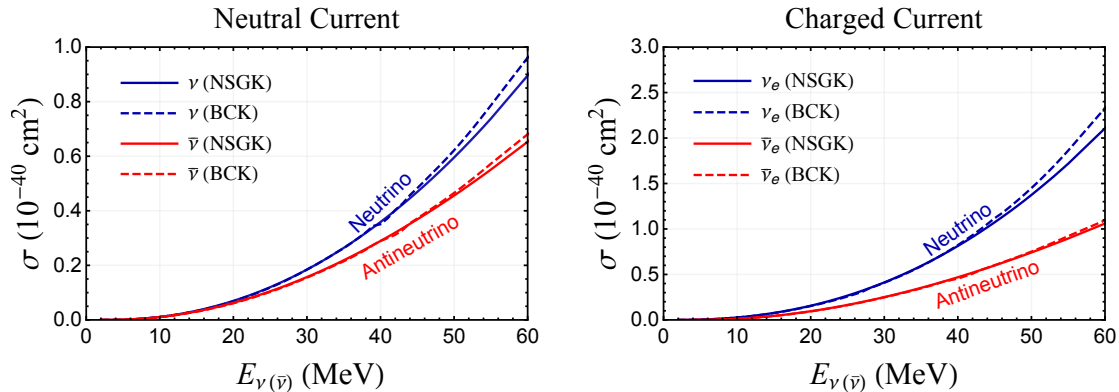


**Figure 1:** The cross section for dissociation of deuteron by neutrino (blue) and antineutrino (red) as a function of incident neutrino or antineutrino energy is shown for Neutral Current (left) and Charged Current (right) interactions. The cross section obtained using PhLA by NSGK [48] is shown by solid lines and the one obtained using  $\not{r}$ EFT by BCK [50] is shown by dashed lines.

obtained and integrated over energy agree with the total cross sections in NSGK to better than a few per cent for neutrino energies up to 50 MeV. This is apparent from Fig. 1. The differential cross sections, thus obtained (see Appendix A for details), are shown in Figure 2 for NC and in Figure 3 for CC interactions. In Appendix B, we provide tabulated NC and CC differential cross sections in terms of the incoming neutrino energy and the *measurable* outgoing proton or electron/positron energy, respectively<sup>5</sup>.

## 2.2 Supernova neutrino fluence and oscillation physics

A supernova emits about 99% of its gravitational binding energy into neutrinos over about 10 seconds [51]. Predicting the neutrino output of a wide range of supernovae remains an outstanding problem in astrophysics [52]. To obtain an estimate of the total events in our detector, we use a provisional model of the supernova neutrino fluence, where the spectral number-fluence for flavor  $\alpha$  is [53]

$$F_{\alpha}^{(0)} = \frac{2.35 \times 10^{13}}{\text{cm}^2 \text{ MeV}} \cdot \left( \frac{\mathcal{E}_{\alpha}}{10^{52} \text{ erg}} \right) \cdot \left( \frac{10 \text{ kpc}}{d} \right)^2 \cdot \frac{E_{\alpha}^3}{\langle E_{\alpha} \rangle^5} \cdot \exp \left( -\frac{4E_{\alpha}}{\langle E_{\alpha} \rangle} \right). \quad (2.1)$$

Here,  $\mathcal{E}_{\alpha}$  is the net energy emitted per flavor,  $d$  is the distance to the supernova, and  $E_{\alpha}$  (and  $\langle E_{\alpha} \rangle$ ) are neutrino energies (and their averages) in MeV [41]. Note that the spectral number-fluence  $F$  gives the number of neutrinos reaching the detector per unit surface area per unit neutrino energy, *without* including effects of flavor conversion.

For our numerical estimates we assume equipartition of energies between all flavors, with  $\mathcal{E}_{\alpha} = 5 \times 10^{52}$  erg for all flavors. The distance  $d$  is taken as 10 kpc. The

<sup>5</sup>Tabulated differential and total cross sections are also available at <https://github.com/bhvzchhn/NeutrinoDeuteron/>.

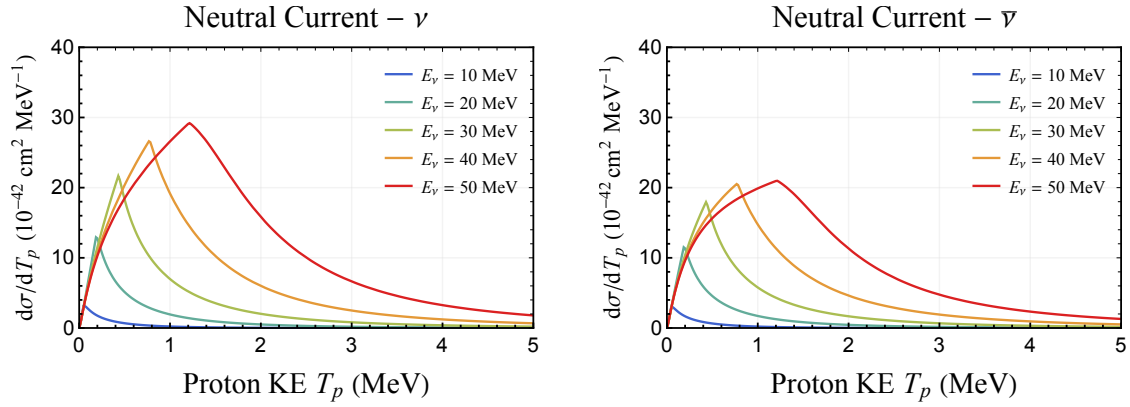


**Figure 2:** The differential cross section for dissociation of deuteron by neutrino (left) and antineutrino (right) for the Neutral Current interaction channel as a function of kinetic energy of final state proton is shown for various choices incident neutrino or antineutrino energy. The difference between neutrino and antineutrino interaction strengths (arising from the sign of  $W_3$  term in Eq.(A.3)) is apparent. One can also infer that the proton carries only a fraction of incident energy, while the majority is carried away by the final state neutrino which is unmeasurable.

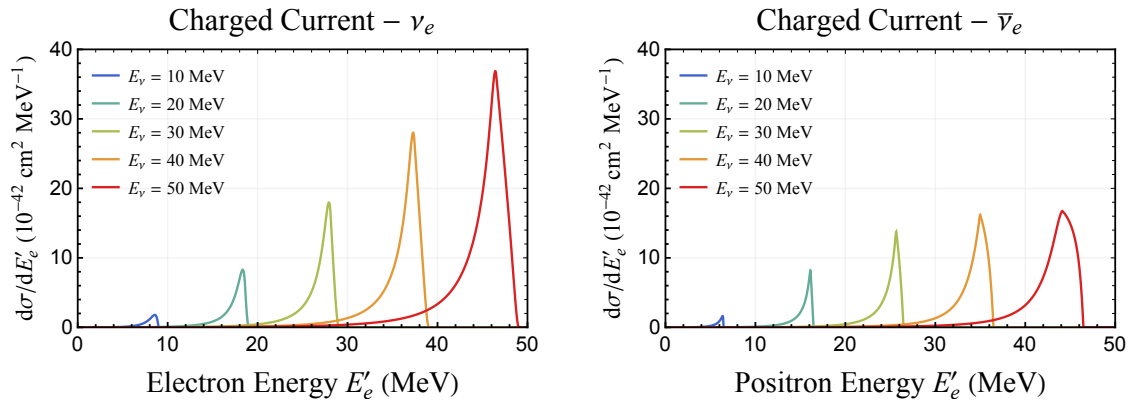


**Figure 3:** The differential cross section for dissociation of deuteron by neutrino (left) and antineutrino (right) for the Charged Current interaction channel as a function of final state charged lepton energy is shown for various choices incident neutrino or antineutrino energy. The difference between neutrino and antineutrino interaction strengths (arising from the sign of  $W_3$  term in Eq.(A.3)) is apparent. At these energies, only the electron flavor participates in these interactions. One can infer that final state lepton carries a significant portion of the incident energy.

values of  $\langle E_\alpha \rangle$  are model dependent and we take two sets of benchmark values for our analysis as outlined in Table 2. The optimistic model, with larger values of  $\langle E_\alpha \rangle$ , gives a higher event rate and is dubbed as High in this paper. A relatively conservative model, with smaller values of  $\langle E_\alpha \rangle$ , gives a lower event rate and is dubbed as Low.

We now include the effects of neutrino oscillations and flavor conversions. We assume that the  $\mu$  and  $\tau$  flavors inside a supernova are identical, and thus the relevant conversion is between the  $e$ -flux and that of some combination of  $\mu$  and  $\tau$ , which we denote as  $x$  [54]. The flavor-converted  $\nu_e$  fluence at Earth can be written as

$$F_e = p F_e^{(0)} + (1 - p) F_x^{(0)}, \quad (2.2)$$

where  $p$  is the net survival probability of  $\nu_e$  from its production to detection. For  $\bar{\nu}_e$ , one has the analogous expression with  $\bar{p}$ ,

$$F_{\bar{e}} = \bar{p} F_{\bar{e}}^{(0)} + (1 - \bar{p}) F_{\bar{x}}^{(0)}. \quad (2.3)$$

For the NC events these oscillations make no difference. However, the CC events are sensitive to  $p$  and  $\bar{p}$ .

We will show our results for two oscillation scenarios: *no oscillation*, where the fluences remain unaltered and one has  $p = 1$  and  $\bar{p} = 1$ , and *flavor equilibrium*, where  $F_\alpha = \frac{1}{3} (F_e^{(0)} + F_\mu^{(0)} + F_\tau^{(0)})$  so that  $p = \frac{1}{3}$  and  $\bar{p} = \frac{1}{3}$ . The former is not physically realizable because MSW effects are guaranteed [55]. However, collective oscillations [56–59] inside the star lead to intricate redistribution of flavor across all energies [60–62], perhaps even to almost complete depolarization (i.e., equilibration between flavors) limited by conservation of lepton numbers [63, 64]. We sidestep the complexities by restricting ourselves to a parametric study. For any other oscillation scenario defined by the respective energy-dependent values of  $p$  and  $\bar{p}$ , one can obtain the predictions by linearly combining the results of these two scenarios as

$$F_e = \frac{3}{2}(1 - p) F_e^{\text{fl. eqbm.}} + \frac{1}{2}(3p - 1) F_e^{\text{no osc.}} \quad (2.4)$$

and

$$F_{\bar{e}} = \frac{3}{2}(1 - \bar{p}) F_{\bar{e}}^{\text{fl. eqbm.}} + \frac{1}{2}(3\bar{p} - 1) F_{\bar{e}}^{\text{no osc.}}. \quad (2.5)$$

### 3 Total number of events

For NC interaction, i.e.,  $\bar{\nu} d \rightarrow \bar{\nu} np$ , the final state neutrino carries a large fraction of the incident neutrino energy but cannot be detected as it does not further interact

**Table 2:** Numerical values of  $\langle E_\alpha \rangle$  in MeV for the neutrino flavors for two benchmark models of supernova neutrino fluence. The model dubbed High is an optimistic choice with larger event rate, compared to Low which is a conservative choice for  $\langle E_\alpha \rangle$ .

Fluence Model	$\langle E_{\nu_e} \rangle$	$\langle E_{\bar{\nu}_e} \rangle$	$\langle E_{\nu_x, \bar{\nu}_x} \rangle$
High (optimistic)	12	15	18
Low (conservative)	10	12	15

inside the detector. The final state neutron and proton have kinetic energy that is approximately

$$T_{n(p)} \sim \frac{E_\nu^2}{M_{n(p)}} \approx 240 \text{ keV} \left( \frac{E_\nu}{15 \text{ MeV}} \right)^2. \quad (3.1)$$

The neutron can be captured on a nucleus, but its energy cannot be reconstructed. However, it allows one to count the total number of NC events which is given by

$$\mathcal{N}_{\text{NC}} = N_d \Delta t \epsilon_n \int_0^\infty dE'_\nu \int_0^\infty dE_\nu \frac{d\phi}{dE_\nu} \frac{d\sigma_{\text{NC}}}{dE'_\nu}, \quad (3.2)$$

where  $N_d$  is the number of deuterons in the detector,  $\epsilon_n$  is the efficiency of neutron capture, and  $\phi$  is the time-averaged neutrino flux with the dimensions of  $\text{cm}^{-2}\text{s}^{-1}$  over the duration of supernova neutrino emission,  $\Delta t \approx 10 \text{ s}$ . In terms of the fluence ( $F \equiv \Delta t \times d\phi/dE_\nu$ ), we can write

$$\mathcal{N}_{\text{NC}} = N_d \int_0^\infty dE_\nu F \sigma_{\text{NC}}, \quad (3.3)$$

which can be evaluated using the tabulated values of the cross section by NGSK [48]. We assume that the neutron capture efficiency is  $\epsilon_n = 1$ . We discuss this assumption in more detail in Section 6. The quenched scintillation signal from the proton can be detected and carries spectral information, but only a fraction of these events will be above the threshold. This is studied in detail in Section 4.1.

For CC interactions, we can not only reconstruct the electron and positron energy, but also the interaction point inside the detector. The binned event rate can be used to obtain the shape of the incoming neutrino spectrum. The number of events in a bin  $j$  is,

$$\mathcal{N}_j = N_d \Delta t \int_{\Delta E'_e} dE'_e \epsilon_e \left[ \int_0^\infty dE_\nu \frac{d\phi}{dE_\nu} \frac{d\sigma_{\text{CC}}}{dE'_e} \right], \quad (3.4)$$

where  $\epsilon_e$  is the efficiency of detecting the electrons. For the remainder of the discussion, we have not included the detector effects and assume  $\epsilon_e = 1$ .

Instead of binned events, one can ask the total number of CC events that will be observed by such a detector. Even though  $E'_e$  depends on  $E_\nu$ , one can carefully use the expression

$$\mathcal{N}_{\text{CC}} = N_d \Delta t \int_0^\infty dE'_e \int_0^\infty dE_\nu \frac{d\phi}{dE_\nu} \frac{d\sigma_{\text{CC}}}{dE'_e} \equiv \sum_j \mathcal{N}_j, \quad (3.5)$$

to calculate the total number of events. After accounting for the kinematic limits, one can write  $\mathcal{N}_{\text{CC}}$  in terms of fluence as,

$$\mathcal{N}_{\text{CC}} = N_d \int_0^\infty dE_\nu F \sigma_{\text{CC}}, \quad (3.6)$$

which is similar to the one obtained for NC interaction (3.3). One can use the tabulated cross-sections in NSGK [48] to estimate the event rates.

Important interactions of neutrino with the deuteron in a DLS are mentioned in the Table 3. The number of target particles ( $N_d$ ) is given for 1 kton of detector volume (see Appendix C for estimates). Although the flux of neutrinos from supernova typically peaks around 10 MeV, the cross section approximately scales as  $E_\nu^{2.5}$  and most of the events arise from  $E_\nu \sim 20$  MeV. We have mentioned the cross section for the interaction channel at 20 MeV to understand their relative strengths.

We have reported the forecasted NC and CC event rates for the “no oscillation” and “flavor equilibrium” scenarios in Tables 4 and 5. For NC interaction, we see that the total number of events remains unchanged and are independent of the oscillation scenario. For CC interaction, the events are larger as we move away from the no oscillation scenario because of the following reason. The  $\nu_{\mu,\tau}$  are emitted at a slightly larger temperature and a fraction of these are converted to  $\nu_e$  due to oscillations. As the interaction cross section increases with neutrino energy, a significant number of events is obtained from these neutrinos. Similar event rates for SNO were estimated in Ref. [65].

As noted before, one can easily use these event rates to get the results for any other oscillation scenario. For example, with only adiabatic MSW effects in the inverted (or normal) mass ordering [55], one has  $p = \sin^2 \theta_{13} \approx 0.02$  (or  $\cos^2 \theta_{13} \sin^2 \theta_{12} \approx 0.3$ ) and  $\bar{p} = \cos^2 \theta_{13} \cos^2 \theta_{12} \approx 0.68$  (or  $\sin^2 \theta_{13} \approx 0.02$ ) [39]. The relevant event rates can be found by combining the “no oscillation” and “flavor equilibrium” event rates using Eqs. (2.4) and (2.5). For example, with fluence model High, one finds 197 (172) CC events for  $\nu_e$  and 99 (81) events for  $\bar{\nu}_e$ .

## 4 Energy spectrum of events

In the previous section, we have seen that the 1 kton of DLS can see several hundreds of neutrino events from a supernova in the galaxy. We have also mentioned that the interactions of the neutrino on deuteron have unique signatures and one can distinguish the events. In this section, we look at the spectrum of events for each channel.

**Table 3:** Representative cross sections for the four neutrino induced deuteron dissociation channels along with their Q values.

Interaction	Channel	-Q (MeV)	$\sigma(E_\nu = 20 \text{ MeV})$
$\nu + d \rightarrow \nu + n + p$	NC	2.224	$6.98 \times 10^{-42} \text{ cm}^2$
$\bar{\nu} + d \rightarrow \bar{\nu} + n + p$	NC	2.224	$6.28 \times 10^{-42} \text{ cm}^2$
$\nu_e + d \rightarrow e^- + p + p$	CC	1.442	$15.61 \times 10^{-42} \text{ cm}^2$
$\bar{\nu}_e + d \rightarrow e^+ + n + n$	CC	4.028	$9.54 \times 10^{-42} \text{ cm}^2$

**Table 4:** Number of NC events for each flavor in 1 kton of DLS from a fiducial supernova at 10 kpc. The event numbers for individual flavors are not observable (as they cannot be distinguished) but provided to allow cross checks, and one only measures the total. The subscript  $x$  refers to any of  $\mu, \tau$ ; note that the  $\bar{\nu}_x$  event rates are slightly lower owing to their smaller NC cross section. The events are reported for different scenarios depending on high / low fluence model and no oscillation / flavor equilibrium case.

Scenario	$\nu_e$	$\bar{\nu}_e$	$\nu_x$	$\bar{\nu}_x$	Total (rounded off)
High; no oscillation	48.4	59.7	88.1	75.6	435
High; flavor equilibrium	74.8	70.3	74.8	70.3	435
Low; no oscillation	36.1	43.7	67.8	59.7	335
Low; flavor equilibrium	57.3	54.3	57.3	54.3	335

**Table 5:** Number of CC events for  $\nu_e$  and  $\bar{\nu}_e$  in 1 kton of DLS from a fiducial supernova at 10 kpc. The two flavors can, in principle, be distinguished in the detector by tagging the hadrons in the final state. The events are reported for different scenarios depending on high / low fluence model and no oscillation / flavor equilibrium case.

Scenario	$\nu_e$	$\bar{\nu}_e$
High; no oscillation	111	90
High; flavor equilibrium	170	108
Low; no oscillation	84	63
Low; flavor equilibrium	130	81

#### 4.1 Neutral current interactions

The NC mediated neutrino dissociation of the deuteron is given by the reaction

$$\bar{\nu}^{(-)} + d \rightarrow \bar{\nu}^{(-)} + n + p, \quad (4.1)$$

where  $\bar{\nu}^{(-)}$  includes all three flavors of (anti)-neutrino. The neutron in the final state leads to observable photons via neutron capture, and we used it to estimate the total event rate. Now we focus on the proton.

##### 4.1.1 Quenched proton spectrum

The final state proton loses its kinetic energy mainly due to ionization energy losses which is converted into scintillation photons in the detector (cross section for the alternate process, capture of proton on deuteron emitting 5 MeV gamma rays, is small [66] and the event rate is negligible). The total amount of scintillation light is not the same as the total kinetic energy due to photo-saturation of the detector, also known as *quenching*. Beacom, Farr, and Vogel (BFV) [40] proposed that the quenched proton signal from neutrino proton elastic scattering can be used to detect supernova

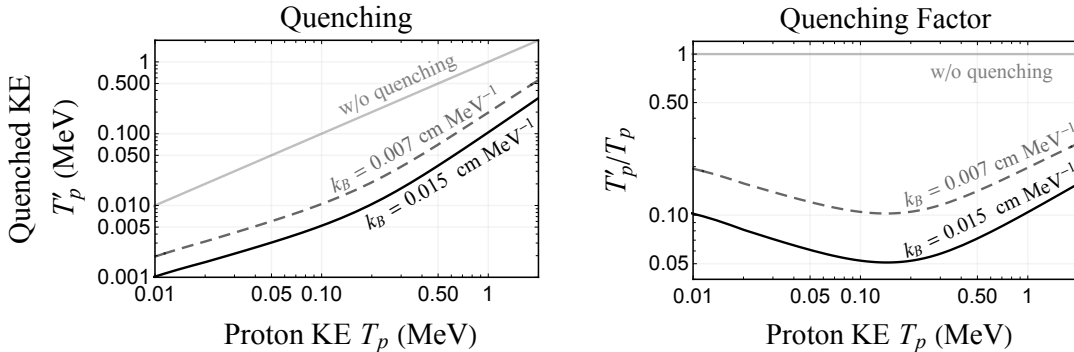


**Figure 4:** The quenched kinetic energy (left) and the quenching factor (right) is shown as a function of the proton energy for two benchmark values of the Birks constant. The solid curve is for  $k_B = 0.015 \text{ cm MeV}^{-1}$  and the dashed curve for  $k_B = 0.007 \text{ cm MeV}^{-1}$ . We also show the unquenched scenario  $T'_p = T_p$ .

neutrinos in scintillation detector such as KamLAND and Borexino. A method for reconstructing the supernova spectrum was proposed in [41]. See also Refs. [67–70].

In contrast to BFV, where there was only one hadron in the final state, here one has an additional particle, a neutron, in the final state. If the scintillation from the proton can be tagged using the  $\gamma$  photons from the neutron capture, one can achieve significant reduction in backgrounds. Moreover, the kinematics of the outgoing proton is not identical to that in BFV as this channel has a three-body final state. However, a simplification is possible if the deuteron breakup occurs in two stages -  $\nu d \rightarrow \nu(d^* \rightarrow np)$  where  $d^*$  is an unstable excited state of the deuteron. In this picture, one can neglect the difference between proton and the neutron, as  $T_p - T_n \ll M_d$ . We have checked that the differential cross section obtained by this method agrees with the plots presented by NSGK.

The differential cross section with respect to the proton recoil energy ( $T_p$ ) can be obtained using

$$\frac{d\sigma}{dT_p} = \left| \frac{\partial E'_\nu}{\partial T_p} \right| \frac{d\sigma}{dE'_\nu}, \quad (4.2)$$

where we use the energy conservation relation  $E'_\nu = E_\nu - B - 2T_p$  and  $B = 2.223 \text{ MeV}$  is the binding energy of the deuteron. The numerical values of the differential cross section for the relevant range of values of  $E_\nu$  are tabulated in Appendix B.

A proton with recoil energy  $T_p$  will lose energy in the detector due to collisions with electrons and the nucleus. It is seen that in typical materials the energy loss rate is dominated by scattering with electrons and approximately is  $(60 - 300) \text{ MeV/cm}$  for  $T_p \approx \text{few MeV}$ . Accurate numerical values for the energy loss rate can be obtained from the PSTAR database<sup>6</sup> for various targets. Similar data can also be obtained using

<sup>6</sup>[www.physics.nist.gov/PhysRefData/Star/Text/PSTAR.html](http://www.physics.nist.gov/PhysRefData/Star/Text/PSTAR.html)

SRIM<sup>7</sup> [71]. Only a small part of the recoil energy, as compared to that of an electron of the same energy, is converted into scintillation light. This electron equivalent quenched kinetic energy  $T'_p$  is given by

$$T'_p = Q(T_p) = \int_0^{T_p} \frac{dT}{1 + k_B \langle dT/dx \rangle}, \quad (4.3)$$

where  $k_B \approx 0.015 \text{ cm MeV}^{-1}$  is the Birks constant [72] and  $\langle dT/dx \rangle$  is the average stopping power that depends on  $T_p$ . For an accurate estimate, one must take the weighted average energy loss due to carbon and deuterium. Unfortunately, the stopping power of deuterium is not known and we approximate it by the stopping power of hydrogen. The stopping power of  $C_n D_{2n}$  is thus taken to be

$$\left\langle \frac{dT}{dx} \right\rangle = \sum_i w_i \left\langle \frac{dT}{dx} \right\rangle_i \approx 0.749 \left\langle \frac{dT}{dx} \right\rangle_C + 0.251 \left\langle \frac{dT}{dx} \right\rangle_H. \quad (4.4)$$

The Birks constant for DLS is also unknown and hence taken to be of same order as other scintillator materials. The quenching factor also depends on the density of the medium which is also an unknown. For simplicity, we assume it to be  $1 \text{ g/cm}^3$  and note that the change due to density can be effectively captured by changing the Birks constant. In Figure 4 we have shown the quenched kinetic energy of the proton for two choices  $k_B = 0.007 \text{ cm MeV}^{-1}$  and  $k_B = 0.015 \text{ cm MeV}^{-1}$ . To obtain conservative estimates of the event rates, we have used the latter for remainder of this paper.

We can now estimate the quenched proton event spectrum using,

$$\frac{d\mathcal{N}}{dT'_p} = \frac{N_d}{dT'_p/dT_p} \int_0^\infty dE_\nu F \frac{d\sigma}{dT_p}, \quad (4.5)$$

where the differential cross section is estimated using Eq. (4.2). In Figure 5 we have shown the differential event rate with proton recoil energy  $T_p$  as well as the quenched kinetic energy  $T'$ . The binned event rate ( $\Delta E_{\text{bin}} = 0.1 \text{ MeV}$ ) with proton recoil energy  $T_p$  and the quenched kinetic energy  $T'_p$  is also shown.

In ordinary scintillator detectors, the dominant background at these energies comes from the beta decay of  $^{14}\text{C}$ . The low energy electrons (up to 200 keV) can mimic the proton scintillation signal. The typical event rate for these backgrounds is  $\mathcal{O}(10^7)$  events per day. Hence, we consider a threshold of 0.2 MeV similar to Ref. [41] to get rid of these backgrounds. One must note that the electron scintillation will not have an accompanying neutron capture signal. Hence these background events can, in principle, be distinguished from the signal events using appropriate tagging. This will lower the threshold and allow for better signal to noise ratio. For a DLS, dedicated study of backgrounds is needed. In Table 6, we have shown the events for the proton recoil via NC channel for various thresholds for both quenched and unquenched spectrum.

---

<sup>7</sup>[www.srim.org](http://www.srim.org)

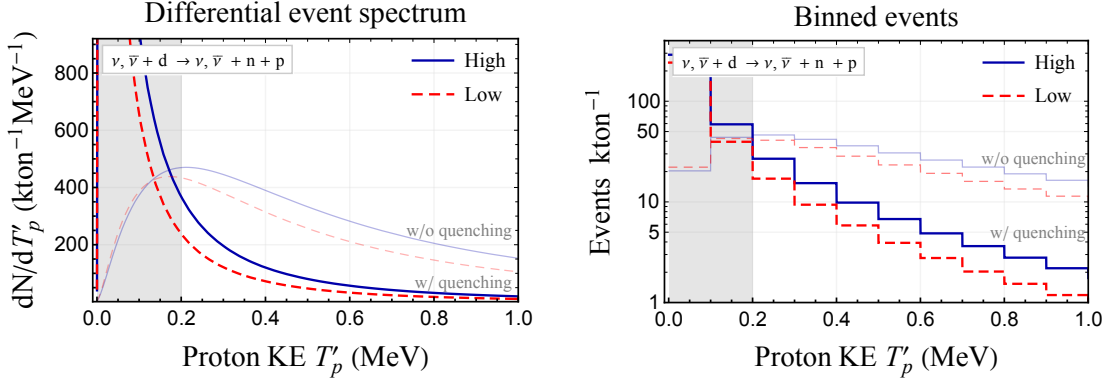


**Figure 5:** The differential event spectrum (left) and binned events (right) with proton recoil energy with and without quenching are shown. The solid blue curves are for optimistic fluence model High and dashed red curves are for the conservative fluence model Low. The gray shading shows energies below threshold, where we take  $E_{th} = 200$  keV due to  $^{14}\text{C}$  beta decay background. However, this threshold can be lowered by tagging the final state neutron.

**Table 6:** Total number of NC events per kton, without quenching ( $T'_p = T_p$ ) and with quenching ( $T'_p = Q(T_p)$ ), for three choices of energy threshold  $E_{th} = 10$  keV, 100 keV, and 200 keV. The neutrino and antineutrino event rates are different, owing to their different cross sections in addition to the difference in fluxes of  $\nu_e$  and  $\bar{\nu}_e$ , but only the total is observable. The energy spectra are shown in Figure 5. The results depend on the fluence model but not on the oscillation scenario.

Fluence model	Flavor	Events/kton without quenching			Events/kton with quenching		
		$E_{th} = 10 ; 100 ; 200$ (keV)			$E_{th} = 10 ; 100 ; 200$ (keV)		
High	$\nu_i$	74.7 ; 71.3 ; 64.0			64.6 ; 25.0 ; 14.8		
	$\bar{\nu}_i$	69.4 ; 66.3 ; 59.4			60.0 ; 22.7 ; 13.3		
	Total	432.4 ; 412.8 ; 370.3			373.8 ; 143.2 ; 84.2		
Low	$\nu_i$	56.7 ; 53.1 ; 46.1			46.6 ; 15.4 ; 8.6		
	$\bar{\nu}_i$	53.4 ; 50.0 ; 43.2			43.7 ; 14.2 ; 7.9		
	Total	330.6 ; 309.3 ; 268.0			271.2 ; 89.0 ; 49.4		

## 4.2 Charged current interactions

As mentioned earlier, due to kinematic threshold only the electron flavor neutrino and antineutrino participate via CC interaction for supernova neutrinos. The final state for  $\nu_e$  is different from  $\bar{\nu}_e$  and the two interaction channels can be distinguished by appropriate tagging. Hence, unlike the NC case, the two flavors are discussed separately as follows.

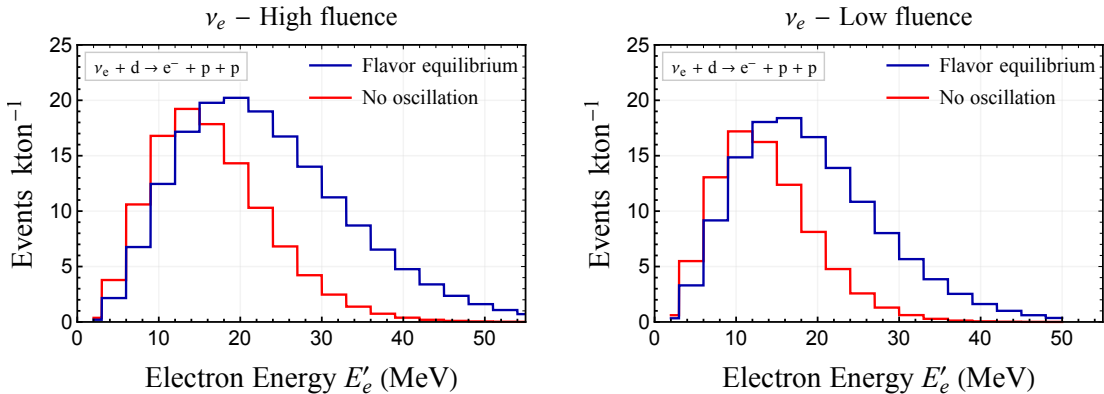


**Figure 6:** Binned event spectrum for  $\nu_e$  detected via Charged Current interactions, with respect to the electron energy. The spectrum assuming flavor equilibrium (no oscillation) is shown with blue (red) lines. Results are shown for the optimistic fluence model High (left) and conservative model Low (right).

#### 4.2.1 CC interaction of $\nu_e$

The CC mediated  $\nu_e$ -deuteron interaction is given by

$$\nu_e + d \rightarrow e^- + p + p, \quad (4.6)$$

where the final state electron is observed through its scintillation radiation. One can, in principle, reconstruct the interaction point by analysing the lepton observed by the PMTs and recover spectral information of the incident neutrino. Hence this channel is important for reconstructing the supernova neutrino spectrum. The two recoiling protons will generate a quenched scintillation signal as well. It seems, a priori, that the signals will overlap and it will be challenging to segregate and tag the events. A quantitative estimate of required detector resolution calls for detailed numerical simulations that is beyond the scope of this paper and we encourage further investigations.

We estimate the event rate binned with respect to observable electron energy. The bin size,  $\Delta E_{\text{bin}} = 3$  MeV, is chosen slightly larger than the expected energy resolution so that the bins are uncorrelated. We show the results in Figure 6 for the two fluence models considered in this paper. It must be noted here that DLS can provide excellent resolution of this channel, both in energy and time, that can only be achieved by a LAr detector such as DUNE. During the 15-20 ms of the neutronization burst, we expect 4.5 (1.5) events from this channel for the no oscillation (flavor equilibrium) scenario. The details are in Appendix D.

#### 4.2.2 CC interaction of $\bar{\nu}_e$

The CC mediated  $\bar{\nu}_e$ -deuteron interaction is given by

$$\bar{\nu}_e + d \rightarrow e^+ + n + n, \quad (4.7)$$

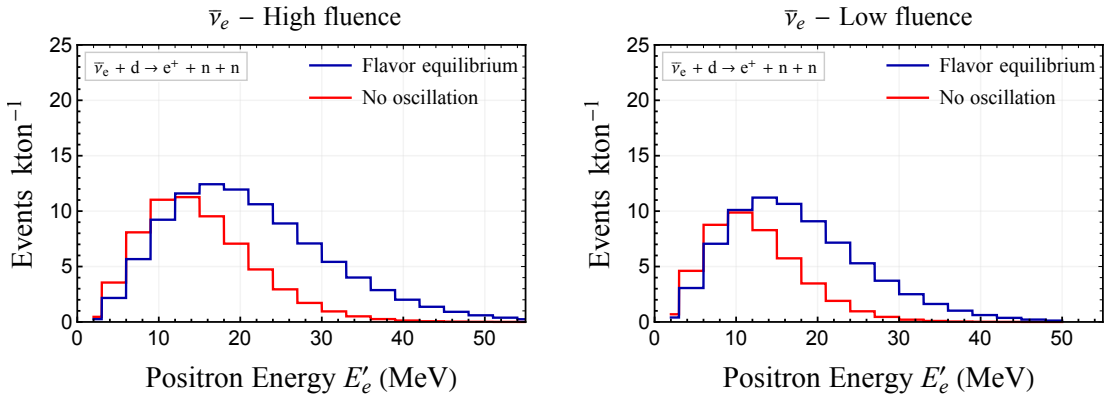


**Figure 7:** Binned event spectrum for  $\bar{\nu}_e$  detected via Charged Current interactions, with respect to the positron energy. The spectrum assuming flavor equilibrium (no oscillation) is shown with blue (red) lines. Results are shown for the optimistic fluence model High (left) and conservative model Low (right).

where the final state positron can be observed through its scintillation. The two neutrons in the final state will thermalize with the medium and their capture will give detectable photons. In principle, the simultaneous observation of these neutrons will provide a cleaner tag for the event compared to the inverse beta decay reaction of  $\bar{\nu}_e$  on a free proton. We have shown the binned event spectrum for this interaction in Figure 7.

### 4.3 Elastic scattering off electrons

The elastic scattering (ES) of neutrinos off electrons in the detector is an important channel to measure NC events in detectors that mostly rely on IBD. In DLS, we expect an aggregate of 15 events, mostly in the lower energy bins due to zero threshold of the interaction. Unlike the NC interaction with deuteron, the ES channel is sensitive to flavor conversion as the cross sections for electron and non-electron flavors are different [73]. In figure 8, we have shown the binned spectrum of events for the two fluence models considered in this paper. The scintillation from recoiling electrons could be considered as a *background* for reconstruction of the incident neutrino spectrum from the CC channel discussed in 4.2.1.

## 5 Secondary interactions

So far, we have focused on neutrinos scattering with deuteron which leads to protons and neutrons in the final state. We have assumed that the protons lead to detectable scintillation, and all of the neutrons are captured and detected. Due to their large energy loss rate, mainly due to ionization, the protons travel  $\mathcal{O}(0.1)$  mm in the detector. On the other hand, the neutrons undergo multiple scatterings off the neighboring nuclei before getting captured, resulting in a  $\mathcal{O}(100)$  cm diffusion length in a DLS. In this section, we explore the role of these recoiling neutrons and the possibility of causing a

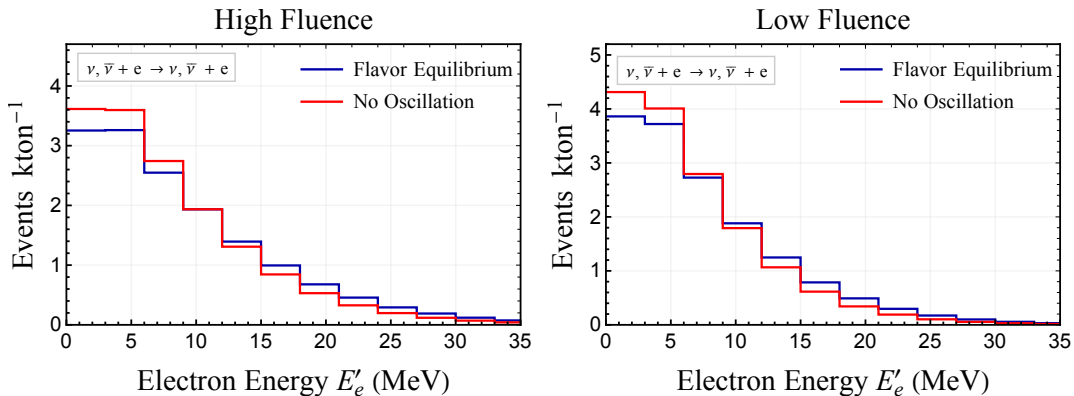


**Figure 8:** Binned event spectrum for elastic scattering off electrons with respect to the measured electron energy. Results are shown for the optimistic fluence model High (blue) and conservative model Low (red). Both models results in an aggregate of approximately 15 events.

dissociation of the deuteron inducing secondary interactions<sup>8</sup>. In the presence of Gd, the neutron is almost immediately captured and secondary interactions are negligible.

In a 100% deuterated scintillator without Gd, the thermal neutron can be captured on deuteron ( $\sigma(n+d \rightarrow {}^3\text{H}+\gamma) = 0.5$  mb) or carbon ( $\sigma(n+{}^{12}\text{C} \rightarrow {}^{13}\text{C}+\gamma) = 3.5$  mb). Using the elastic scattering cross sections of  $\mathcal{O}(1)$  b, one can estimate that the recoiling neutron undergoes  $\mathcal{O}(1000)$  scatterings off deuteron and carbon before getting captured. A fraction of these neutrons having kinetic energy larger than deuteron binding energy can dissociate the deuteron ( $\sigma(n+d \rightarrow n+n+p) = 250$  mb)[74]. In Figure 9, we have shown the distribution of recoiling neutron kinetic energy for various scenarios considered in this paper. We have explicitly shown the count of neutrons having kinetic energy above the deuteron breakup threshold as well as the count above twice the threshold. Depending on the fluence model and flavor conversion scenario, one expect 35-70 (approximately 10% of the event rate) neutrons that can break up the deuteron. These secondary interactions cannot be distinguished from neutrino induced dissociation and would be considered as *background* during reconstruction. The recoiling deuteron from  $n-d$  elastic scattering would, in principle, lead to scintillation signal. However, the average momentum transfer will be close to or below the detection threshold.

The problem of secondary neutrons originates from the low capture efficiency of deuteron, and to a lesser extent of carbon. Assuming partial deuteration results in a significant number of free protons in the DLS. As the cross section for neutron capture on proton is about 650 times larger ( $\sigma(n+p \rightarrow {}^3\text{H}+\gamma) = 330$  mb), one anticipates that a significant fraction of the neutrons would be captured before they can dissociate the deuteron. However, having free protons introduces an additional problem of

<sup>8</sup>We thank the anonymous referee for pointing out this issue.

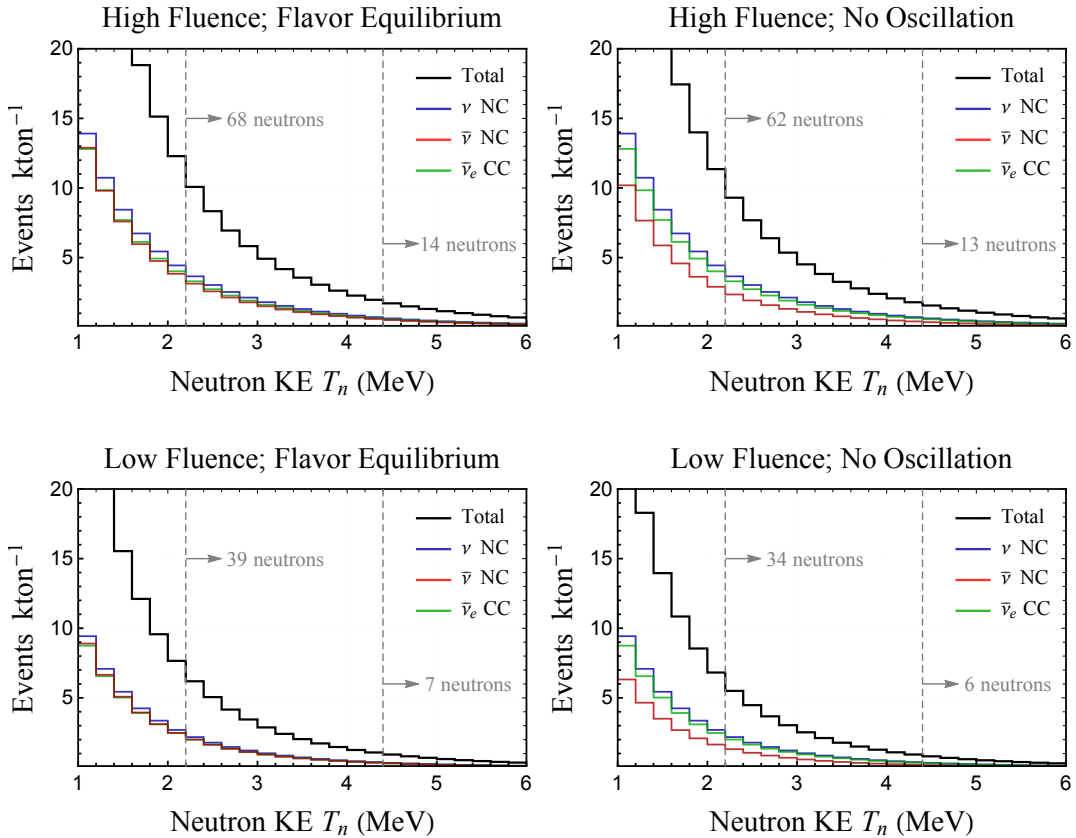


**Figure 9:** The spectrum of events with respect to the kinetic energy of the recoiling neutron is shown for choices of fluence parameters (High and Low) and flavor conversion scenario (flavor equilibrium and no oscillation) considered in this paper. We have shown the count of neutrons having kinetic energy above the deuteron breakup threshold as well as the count above twice the threshold.

segregating elastic scattering on proton ( $\nu, \bar{\nu} + p \rightarrow \nu, \bar{\nu} + p$ ) from the NC dissociation ( $\nu, \bar{\nu} + d \rightarrow \nu, \bar{\nu} + p + n$ ) where the neutron is not detected. In addition, having lesser target deuterons would reduce the expected signal as well.

The problem of accounting for secondary interactions can be circumvented if one adds Gd to the detector. The neutron capture cross section on Gd is extremely large<sup>9</sup> ( $\sigma(n + {}^{155,157}\text{Gd} \rightarrow {}^{156,158}\text{Gd} + \gamma) = 61100 \text{ b}, 254000 \text{ b}$  respectively). As a consequence, for 0.1% concentration of Gd, the dominant interaction of recoiling neutrons would be on Gd and they get captured before elastic/inelastic scatterings can take place. We note that neutron time of flight measurements using LAPPD<sup>10</sup> can, in principle, identify the secondary interactions.

<sup>9</sup>The natural abundance of  ${}^{155}\text{Gd}$  and  ${}^{157}\text{Gd}$  are 14.8% and 15.6% respectively.

<sup>10</sup>Large Area Picosecond Photo-Detectors [75]

## 6 Summary

In this paper, we have shown the potential of a deuterated liquid scintillator based detector for observing supernova neutrinos. We employed the framework of  $\not\alpha$ EFT to evaluate the cross sections for neutrino dissociation of the deuteron. We checked that the evaluated cross sections are appropriate for supernova neutrino energies and have computed the event rates in 1 kton of DLS. We find that for an optimistic choice of supernova neutrino parameters, one can observe up to 435 NC events, 170  $\nu_e$  and 108  $\bar{\nu}_e$  CC events for a typical galactic supernova at a distance of 10 kpc from Earth. This ability to detect all flavors in a single detector can allow a model-independent determination of the flavor-mixing scenario [76].

We have also looked at the spectrum of events for these interaction channels. For NC, we looked at the quenched scintillation signal from the proton in the final state. We show that, for threshold at 200 keV, one can observe up to 85 scintillation events from the proton. The spectral analysis of these events can, in principle, be used to reconstruct the incident neutrino spectrum. Observation of these NC events will allow for independent normalization of the supernova neutrino flux as well as aid in understanding intricate oscillation physics.

Most of the operational neutrino detectors rely on IBD to detect  $\bar{\nu}_e$ . A DLS is not only sensitive to the elusive  $\nu_e$ , but the cross section for this channel is larger than the other channels. Assuming flavor equilibrium, one obtains up to 170 events for  $\nu_e$  and up to 110 events for  $\bar{\nu}_e$ . These two CC interaction channels have characteristic signature in the detector due to different final state particles. We have also shown the spectrum of these events which can also be used to reconstruct the incident neutrino spectrum.

The  $\gamma$ s from the neutron capture are a prevalent signature in all of the interaction channels except the CC interaction of  $\nu_e$ . This allows reduction of backgrounds *if* the neutron can be tagged. Here we assumed that the thermal neutron always gets captured, which is an excellent assumption in presence of Gd. Without Gd, the neutrons have a large diffusion length and might escape the detector. The neutron capture efficiency is also enhanced, if the detector will have some fraction of free protons due to partial deuteration of the scintillator. However, this introduces an additional complexity of segregating  $\nu - p$  elastic scattering with  $\nu - d$  NC dissociation where the recoiling neutron escapes undetected. Depending on the technological challenges with manufacture of the Gd doped DLS, as well as its physics performance, suitable optimization is needed, keeping various constraints in mind.

Reconstruction of the neutrino spectrum using the NC events in a DLS based detector will be challenging but important. The key challenge concerns not the quenching [41], but rather the absence of one-to-one correspondence between the incident neutrino energy and the measured proton energy in a three body final state. Never-

theless, the differential scattering cross section is known and can be inverted, as in Ref. [41]. An unfolding based approach, including the detector systematics, may be useful [67–70].

A DLS can also be used to study other aspects of low energy neutrino physics. Our preliminary estimates indicate that a kton of DLS will not be sufficient to observe the diffuse supernova background, given existing constraints from Super-K [77]. It has promising applications in solar neutrino physics where the  $\nu_e$  can be detected at low energies [78]. Moreover, such a detector can also probe beyond standard model physics such as proton decay [79–81], neutrinoless double beta decay [82, 83], and axions from the Sun [84].

The observation of the next galactic supernova promises to significantly improve our understanding of core-collapse supernovae and the nature of its neutrino emission. However, a lot more work remains to be done in simulating supernovae and their neutrino fluxes and in computing the nature of flavor conversions therein. Although we now have several large neutrino detectors capable of detecting supernova neutrinos, substantial efforts are underway to develop adequate detection and analysis strategies [76, 85–87]. It is our understanding that a DLS based detector will greatly aid in this task.

## Acknowledgments

We thank J.W. Chen, for a useful discussion on the  $B_0$  integral and its implementation. We especially thank John Beacom, Amol Dighe, Milind Diwan, Ranjan Laha, M.V.N. Murthy, and R. Palit for valuable comments and suggestions. The work of BD is supported by the Dept. of Atomic Energy (Govt. of India) research project under Project Identification No. RTI 4002, the Dept. of Science and Technology (Govt. of India) through a Swarnajayanti Fellowship, and by the Max-Planck-Gesellschaft through a Max Planck Partner Group.

## A Revisiting neutrino deuteron interactions

The cross section for neutrino dissociation of deuteron can be calculated in two independent ways. In the Phenomenological Lagrangian Approach (PhLA), the nuclear transition matrix elements are obtained using the hadronic currents and the nuclear wave functions. The hadronic currents are obtained with one body currents using impulse approximation and two-body meson exchange currents. The initial and final state nuclear wave functions are obtained by solving the Schrödinger equation for phenomenological nucleon-nucleon (NN) potential. In the paper by Nakamura, Sato, Gudkov, and Kubodera (NSGK) [48], the authors used the Argonne- $v18$  NN potential to obtain the cross section. On the other hand, the cross section can also be calculated in the framework of Pionless Effective Field Theory ( $\not\pi$ EFT) valid for  $E_\nu \ll m_\pi$

[49]. In this approach, the massive hadronic degrees of freedom (for example  $\pi$  and  $\Delta$ ) are considered non-dynamical and integrated out. The nuclear interactions are then calculated perturbatively using the ratio of light and heavy scales as the expansion parameter. The light scales in the theory are determined by the nuclear scattering lengths ( $\sim 10$  MeV) and the deuteron binding momentum ( $\sim 50$  MeV) whereas the heavy scale (also the cut-off) is given by the pion mass ( $m_\pi \sim 100$  MeV). In the paper by Butler, Chen, and Kong (BCK) [50], the authors have obtained neutrino-deuteron cross sections at next-to-next-to-leading-order.

The total cross sections obtained by both methods are in excellent agreement. In PhLA, there are many undetermined form factors whose numerical values are obtained by matching the theory predictions to other experiments (for example, photo-dissociation of deuteron, i.e.,  $d + \gamma \rightarrow n + p$ ). As the parameters are determined by precise experiments, the predictions of neutrino-deuteron cross section in this approach are very robust. Whereas in  $\not\propto$ EFT, there are no undetermined parameters (barring the counter-term  $L_{1,A}$ ), as everything can be systematically obtained starting from Standard Model. On the flip side, PhLA is valid up to very large neutrino energies ( $> 150$  MeV) but  $\not\propto$ EFT starts to become inaccurate at few tens of MeV. In Figure 1 we see that the total cross sections obtained by NSGK and BCK are very similar up to neutrino energy of 50 MeV. Thus we can safely use  $\not\propto$ EFT for estimating the supernova neutrino event rates.

The two approaches are independent and complementary. In order to match the total cross sections with NSGK at a percent level accuracy, the numerical value of the unknown counter term in BCK is obtained in what would be the *natural* range for the parameter. The agreement of these approaches at low energy also serves to validate the approximations made in PhLA.

In the trailing discussion, we outline the relevant results from BCK [50] to correct the above said typo. The differential cross section for neutrino-deuteron interaction is given by

$$\frac{d^2\sigma}{dE'd\Omega} = \frac{G_F^2}{32\pi^2} \frac{\mathbf{k}'}{\mathbf{k}} S_1(\mathbf{k}') \ell_{\mu\nu} W^{\mu\nu} \quad (\text{A.1})$$

where  $\mathbf{k}$  ( $\mathbf{k}'$ ) is the three momentum and  $E$  ( $E'$ ) is the energy of the initial (final) lepton. The Coulomb interaction between final state particles is encapsulated by  $S_1$  which is significant at low energies and thus relevant for supernova neutrino interactions. The lepton current tensor is given by,

$$\ell^{\mu\nu} = 8(k^\mu k'^\nu + k^\nu k'^\mu - k \cdot k' g^{\mu\nu} \pm i\varepsilon^{\mu\nu\rho\sigma} k_\rho k'_\sigma) \quad (\text{A.2})$$

and the hadronic current tensor ( $W_{\mu\nu}$ ) is given in terms of six independent structure functions. Of these, only three ( $W_1$ ,  $W_2$ ,  $W_3$ ) give non-zero contribution. In terms of these, the differential cross section is simplified as,

$$\frac{d^2\sigma}{dE'd\Omega} = \frac{G_F^2 E_\nu \mathbf{k}'}{2\pi^2} S_1(\mathbf{k}') \left[ 2W_1 \sin^2 \frac{\theta}{2} + W_2 \cos^2 \frac{\theta}{2} \mp 2 \frac{(E_\nu + E')}{M_d} W_3 \sin^2 \frac{\theta}{2} \right] \quad (\text{A.3})$$

where the - (+) sign in front of the third term is for (anti-) neutrino in the initial state.

We use the perturbative expressions for the structure functions  $W_{1,2,3}$ , as given in BCK [50]. However, Eq.(53) in BCK, which includes the Coulomb interaction between the final state protons in the CC interaction  $\nu_e + d \rightarrow e + p + p$ , has a typo, where  $k^2$  in the denominator of the last term was mistakenly printed as  $q^2$ . The correct expression is

$$B_0 = M_N \int \frac{d^3k}{(2\pi)^3} \frac{\sqrt{8\pi\gamma}}{k^2 + \gamma^2} \frac{2\pi\eta_k}{e^{2\pi\eta_k} - 1} \frac{e^{2\eta_k \tan^{-1}(k/\gamma)}}{p^2 - k^2 + i\epsilon} \left[ 1 + \frac{\mathbf{q}^2 ((1 - 2\eta_k^2)k^2 - 6\eta_k k\gamma - 3\gamma^2)}{12(k^2 + \gamma^2)^2} \right] \quad (\text{A.4})$$

where  $M_N = 939$  MeV is the mass of a nucleon,  $\gamma = 45.70$  MeV is the deuteron internal momentum, and  $\eta_k = \alpha M_N / (2k)$ . The fine structure constant  $\alpha = 1/137$  at these scales. The magnitude of the relative momentum between the protons is  $2p$  and  $\mathbf{q}$  is the spatial component of the momentum transfer. Substituting for  $\eta_k$ , the expression can be written as

$$B_0 = \frac{M_N \gamma^{1/2}}{2\pi^2} \int_0^\infty dk \frac{k^2}{k^2 + \gamma^2} \frac{C[k]}{p^2 - k^2} \left[ 1 + \frac{\mathbf{q}^2 (2k^2 - M_N^2 \alpha^2 - 6M_N \alpha \gamma - 6\gamma^2)}{24(k^2 + \gamma^2)^2} \right], \quad (\text{A.5})$$

where  $C[k] = (2\pi\eta_k)(e^{2\pi\eta_k} - 1)^{-1} e^{2\eta_k \tan^{-1}(k/\gamma)}$  is related to the Coulomb interaction between the nucleons. This integral must be evaluated carefully: the integrand has poles at  $\pm i\gamma$  and  $\pm p$ , but  $C[k]$  is undefined at  $\pm i\gamma$ ; so, one replaces  $C[k] \rightarrow (C[k] - 1) + 1$ , and the  $k$ -integral involving  $C[k] - 1$  is computed numerically by taking the principal value at  $k = p$ , whereas the latter (for which the integrand is even in  $k$  and vanishes at  $k \rightarrow \infty$ ) is computed using the method of residues. The differential cross sections, thus obtained, are shown in Figure 2 for NC and in Figure 3 for CC interactions.

## B Tabulated differential cross sections

### B.1 $\nu + d \rightarrow \nu + n + p$

**Table 7:** The differential cross section ( $d\sigma/dT_p$  in units of  $10^{-42} \text{ cm}^2 \text{ MeV}^{-1}$ ) for  $\nu$  NC interaction is tabulated for various choices of recoiling proton kinetic energy  $T_p$  and incoming neutrino energy  $E_\nu$ .

$T_p$ (MeV)	$E_\nu = 5$ MeV	10 MeV	15 MeV	20 MeV	30 MeV	50 MeV
0.001	0.032	0.041	0.042	0.043	0.044	0.045
0.01	0.325	0.406	0.420	0.429	0.441	0.452
0.05	0.380	3.161	3.287	3.125	3.038	3.022
0.1	0.289	2.701	7.627	6.731	6.135	5.875
0.2	0.170	1.758	5.556	12.770	11.510	10.260
0.3	0.106	1.228	3.907	8.981	16.190	13.560
0.4	0.068	0.899	2.905	6.635	20.440	16.220
0.5	0.044	0.679	2.239	5.125	18.320	18.470
1.0	0.004	0.214	0.806	1.932	6.977	26.590
2.0	-	0.031	0.184	0.505	2.020	15.830
3.0	-	0.003	0.054	0.180	0.813	6.638
4.0	-	-	0.016	0.072	0.384	3.256
5.0	-	-	0.003	0.030	0.199	1.791
6.0	-	-	-	0.012	0.109	1.066
7.0	-	-	-	0.004	0.061	0.670
8.0	-	-	-	0.001	0.034	0.439
9.0	-	-	-	-	0.019	0.296
10.	-	-	-	-	0.010	0.204
11.	-	-	-	-	0.004	0.142
12.	-	-	-	-	0.002	0.100
13.	-	-	-	-	-	0.071
14.	-	-	-	-	-	0.050
15.	-	-	-	-	-	0.035
16.	-	-	-	-	-	0.024
17.	-	-	-	-	-	0.017
18.	-	-	-	-	-	0.011
19.	-	-	-	-	-	0.007
20.	-	-	-	-	-	0.004
21.	-	-	-	-	-	0.002
22.	-	-	-	-	-	0.001
23.	-	-	-	-	-	-
24.	-	-	-	-	-	-
25.	-	-	-	-	-	-

## B.2 $\bar{\nu} + d \rightarrow \bar{\nu} + n + p$

**Table 8:** The differential cross section ( $d\sigma/dT_p$  in units of  $10^{-42} \text{ cm}^2 \text{ MeV}^{-1}$ ) for  $\bar{\nu}$  NC interaction is tabulated for various choices of recoiling proton kinetic energy  $T_p$  and incoming neutrino energy  $E_\nu$ .

$T_p$ (MeV)	$E_\nu = 5$ MeV	10 MeV	15 MeV	20 MeV	30 MeV	50 MeV
0.001	0.032	0.040	0.042	0.043	0.044	0.045
0.01	0.317	0.400	0.415	0.426	0.439	0.451
0.05	0.372	3.000	3.138	3.011	2.960	2.975
0.1	0.282	2.561	7.026	6.271	5.822	5.684
0.2	0.167	1.667	5.103	11.340	10.400	9.583
0.3	0.104	1.165	3.590	7.980	14.030	12.240
0.4	0.067	0.853	2.669	5.897	17.090	14.170
0.5	0.043	0.644	2.057	4.555	15.170	15.650
1.0	0.004	0.203	0.740	1.715	5.776	19.890
2.0	-	0.030	0.169	0.447	1.668	11.310
3.0	-	0.003	0.049	0.159	0.670	4.750
4.0	-	-	0.014	0.064	0.317	2.334
5.0	-	-	0.003	0.027	0.164	1.287
6.0	-	-	-	0.010	0.090	0.768
7.0	-	-	-	0.003	0.051	0.485
8.0	-	-	-	0.001	0.028	0.319
9.0	-	-	-	-	0.016	0.216
10.	-	-	-	-	0.008	0.150
11.	-	-	-	-	0.004	0.105
12.	-	-	-	-	0.001	0.075
13.	-	-	-	-	-	0.053
14.	-	-	-	-	-	0.038
15.	-	-	-	-	-	0.027
16.	-	-	-	-	-	0.019
17.	-	-	-	-	-	0.013
18.	-	-	-	-	-	0.009
19.	-	-	-	-	-	0.005
20.	-	-	-	-	-	0.003
21.	-	-	-	-	-	0.002
22.	-	-	-	-	-	0.001
23.	-	-	-	-	-	-
24.	-	-	-	-	-	-
25.	-	-	-	-	-	-

### B.3 $\nu_e + d \rightarrow e^- + p + p$

**Table 9:** The differential cross section ( $d\sigma/dE'_e$  in units of  $10^{-42}$  cm<sup>2</sup> MeV<sup>-1</sup>) for  $\nu_e$  CC interaction is tabulated for various choices of outgoing electron energy  $E'_e$  and incoming neutrino energy  $E_\nu$ . The kinematic cut-off  $m_e \leq E'_e \leq E_\nu - 0.93$  MeV is apparent.

$E'_e$ (MeV)	$E_\nu = 5$ MeV	10 MeV	15 MeV	20 MeV	30 MeV	50 MeV
0.5	-	-	-	-	-	-
1.0	0.004	0.001	0.000	0.000	0.000	0.000
2.0	0.034	0.003	0.001	0.000	0.000	0.000
3.0	0.169	0.011	0.003	0.001	0.000	0.000
4.0	0.049	0.029	0.007	0.003	0.001	0.000
5.0	-	0.070	0.013	0.005	0.002	0.000
6.0	-	0.170	0.025	0.009	0.003	0.001
7.0	-	0.439	0.046	0.014	0.004	0.001
8.0	-	1.249	0.084	0.023	0.006	0.001
9.0	-	0.068	0.155	0.037	0.008	0.002
10.	-	-	0.297	0.058	0.011	0.003
11.	-	-	0.606	0.091	0.016	0.003
12.	-	-	1.371	0.146	0.022	0.004
13.	-	-	3.460	0.239	0.029	0.006
14.	-	-	0.064	0.404	0.040	0.007
15.	-	-	-	0.722	0.055	0.009
16.	-	-	-	1.392	0.074	0.011
17.	-	-	-	2.997	0.102	0.013
18.	-	-	-	6.992	0.141	0.016
19.	-	-	-	0.063	0.197	0.020
20.	-	-	-	-	0.280	0.024
21.	-	-	-	-	0.406	0.029
22.	-	-	-	-	0.602	0.035
23.	-	-	-	-	0.925	0.042
24.	-	-	-	-	1.484	0.051
25.	-	-	-	-	2.528	0.062
26.	-	-	-	-	4.676	0.075
27.	-	-	-	-	9.565	0.091
28.	-	-	-	-	15.420	0.111
29.	-	-	-	-	0.063	0.136
30.	-	-	-	-	-	0.167
35	-	-	-	-	-	0.507
40	-	-	-	-	-	2.048
45	-	-	-	-	-	16.880
50	-	-	-	-	-	-

#### B.4 $\bar{\nu}_e + d \rightarrow e^+ + n + n$

**Table 10:** The differential cross section ( $d\sigma/dE'_e$  in units of  $10^{-42}$  cm<sup>2</sup> MeV<sup>-1</sup>) for  $\bar{\nu}_e$  CC interaction is tabulated for various choices of outgoing positron energy  $E'_e$  and incoming neutrino energy  $E_\nu$ .

$E'_e$ (MeV)	$E_\nu = 5$ MeV	10 MeV	15 MeV	20 MeV	30 MeV	50 MeV
0.5	-	-	-	-	-	-
1.0	0.021	0.001	0.000	0.000	0.000	0.000
2.0	-	0.007	0.002	0.001	0.000	0.000
3.0	-	0.023	0.005	0.002	0.001	0.000
4.0	-	0.070	0.011	0.005	0.002	0.001
5.0	-	0.219	0.023	0.008	0.003	0.001
6.0	-	0.896	0.045	0.014	0.005	0.002
7.0	-	-	0.087	0.023	0.007	0.003
8.0	-	-	0.173	0.038	0.010	0.004
9.0	-	-	0.369	0.060	0.014	0.005
10.	-	-	0.907	0.097	0.019	0.006
11.	-	-	3.156	0.159	0.026	0.007
12.	-	-	-	0.269	0.035	0.009
13.	-	-	-	0.483	0.046	0.011
14.	-	-	-	0.946	0.063	0.014
15.	-	-	-	2.168	0.085	0.017
16.	-	-	-	7.180	0.115	0.020
17.	-	-	-	-	0.158	0.024
18.	-	-	-	-	0.220	0.029
19.	-	-	-	-	0.313	0.034
20.	-	-	-	-	0.457	0.041
21.	-	-	-	-	0.689	0.048
22.	-	-	-	-	1.087	0.057
23.	-	-	-	-	1.826	0.067
24.	-	-	-	-	3.366	0.080
25.	-	-	-	-	7.257	0.095
26.	-	-	-	-	9.398	0.113
27.	-	-	-	-	-	0.135
28.	-	-	-	-	-	0.162
29.	-	-	-	-	-	0.196
30.	-	-	-	-	-	0.238
35	-	-	-	-	-	0.712
40	-	-	-	-	-	3.187
45	-	-	-	-	-	14.900
50	-	-	-	-	-	-

## C Estimating the number of target nuclei $N_d$

In this paper, the event rates are obtained for 100% deuterated hydrocarbon of the generic form  $C_nD_{2n}$ . The density is assumed to be  $1 \text{ g/cm}^3$ . The molar mass of such a compound is  $n \times 12.0107 + 2n \times 2.014 \approx 16.04n \text{ g/mol}$ . For 1 kton of detector volume, the number of deuteron targets is

$$N_d = 2n \times \frac{10^9}{16.04n} \times N_A \approx 7.53 \times 10^{31} \quad (\text{C.1})$$

where  $N_A = 6.023 \times 10^{23}$  is the Avogadro's number and the prefactor accounts for the fact that there are  $2n$  deuteron target per molecule of  $C_nD_{2n}$ . One can obtain estimates for carbon and electron as follows.

$$N_{T,C} = \frac{n}{2n} \times N_{T,D} = 3.76 \times 10^{31} \quad (\text{C.2})$$

$$N_{T,e} = 6 \times N_{T,C} + N_{T,D} = 3.00 \times 10^{32} \quad (\text{C.3})$$

One can also consider 100% deuterated linear alkylbenzene ( $C_6D_5C_nD_{2n+1}$ ) based scintillator. For the alkyl group,  $n$  usually lies between 10 and 16. Assuming  $n = 12$ , the number of deuteron targets per kton is

$$N_d^{dLAB} = 30 \times \frac{10^9}{276.61} \times N_A \approx 6.53 \times 10^{31} \quad (\text{C.4})$$

which is about 15% smaller and the event rates will be scaled accordingly.

## D Neutronization Burst

A typical neutronization burst lasts about 15-20 ms with peak luminosity of  $3.3 - 3.5 \times 10^{53} \text{ ergs/sec}$  and is nearly independent of progenitor mass and other parameters [47]. During this burst, not only the luminosity, but also the average energy of the neutrinos changes with time and a simple description, similar to the one we have adopted for fluence, is not sufficient. Deferring details to a future publication, here we show the timing spectra of the events from a neutronization burst. We have adopted the time series of luminosity and average energy from [47] for a  $15 M_\odot$  progenitor, and assume a uniform pinching factor of 3. The events from non-electron flavor neutrinos are negligible. The expected event rate at the detector depends on the neutrino mass hierarchy as well as the flavor conversion parameters. The timing spectrum of events for the two flavor conversion scenarios is shown in Figure 10. For the flavor equilibrium case, the NC events are unchanged and the CC events are scaled by a factor of  $1/3$  as compared to the *no oscillation* scenario. Over the course of the burst, we obtain an aggregate of 6.5 events (2 NC; 4.5 CC) for the no oscillation scenario and 3.5 events (2 NC; 1.5 CC) for the flavor equilibrium scenario.

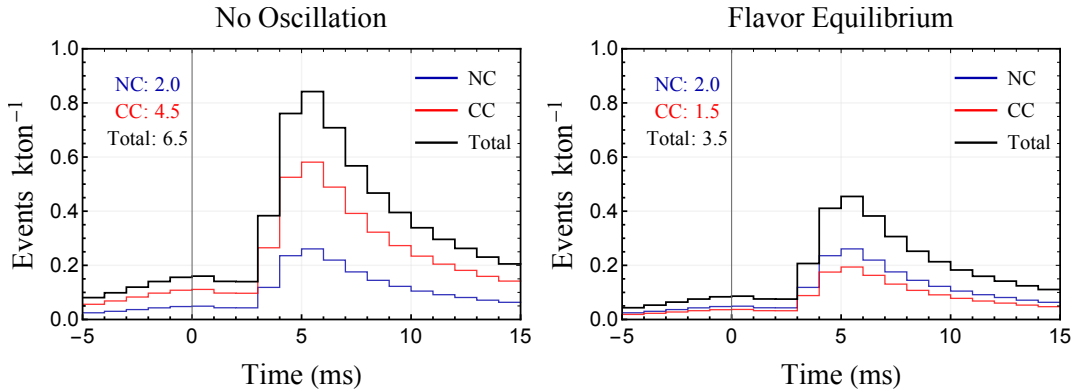


**Figure 10:** The timing spectrum of events during the neutronization burst for the no oscillation (left) and flavor equilibrium (right) scenario. The aggregate event rate over the course of burst is shown as well.

## References

- [1] B. C. Reed, *New estimates of the solar-neighborhood massive-stars birthrate and the Galactic supernova rate*, *Astron. J.* **130** (2005) 1652 [[astro-ph/0506708](#)].
- [2] K. Rozwadowska, F. Vissani and E. Cappellaro, *On the rate of core collapse supernovae in the milky way*, *New Astron.* **83** (2021) 101498 [[2009.03438](#)].
- [3] KAMIOKANDE-II collaboration, K. Hirata et al., *Observation of a Neutrino Burst from the Supernova SN 1987a*, *Phys. Rev. Lett.* **58** (1987) 1490.
- [4] K. S. Hirata et al., *Observation in the Kamiokande-II Detector of the Neutrino Burst from Supernova SN 1987a*, *Phys. Rev. D* **38** (1988) 448.
- [5] R. M. Bionta et al., *Observation of a Neutrino Burst in Coincidence with Supernova SN 1987a in the Large Magellanic Cloud*, *Phys. Rev. Lett.* **58** (1987) 1494.
- [6] E. N. Alekseev, L. N. Alekseeva, V. I. Volchenko and I. V. Krivosheina, *Possible Detection of a Neutrino Signal on 23 February 1987 at the Baksan Underground Scintillation Telescope of the Institute of Nuclear Research*, *JETP Lett.* **45** (1987) 589.
- [7] J. R. Ellis and K. A. Olive, *Constraints on Light Particles From Supernova Sn1987a*, *Phys. Lett. B* **193** (1987) 525.
- [8] S. Cullen and M. Perelstein, *Sn 1987a constraints on large compact dimensions*, *Physical Review Letters* **83** (1999) 268–271.
- [9] G. Raffelt and D. Seckel, *Bounds on Exotic Particle Interactions from SN 1987a*, *Phys. Rev. Lett.* **60** (1988) 1793.
- [10] M. S. Turner, *Axions from SN 1987a*, *Phys. Rev. Lett.* **60** (1988) 1797.
- [11] R. Mayle, J. R. Wilson, J. R. Ellis, K. A. Olive, D. N. Schramm and G. Steigman, *Constraints on Axions from SN 1987a*, *Phys. Lett. B* **203** (1988) 188.
- [12] K. Choi and A. Santamaria, *Majorons and Supernova Cooling*, *Phys. Rev. D* **42** (1990) 293.

- [13] R. Gandhi and A. Burrows, *Massive Dirac neutrinos and the SN1987A signal*, *Phys. Lett. B* **246** (1990) 149.
- [14] J. Arafune and M. Fukugita, *Physical Implications of the Kamioka Observation of Neutrinos From Supernova Sn1987a*, *Phys. Rev. Lett.* **59** (1987) 367.
- [15] W. D. Arnett and J. L. Rosner, *Neutrino Mass Limits From Sn1987a*, *Phys. Rev. Lett.* **58** (1987) 1906.
- [16] E. W. Kolb, A. J. Stebbins and M. S. Turner, *How Reliable Are Neutrino Mass Limits Derived from SN 1987a?*, *Phys. Rev. D* **35** (1987) 3598.
- [17] E. W. Kolb and M. S. Turner, *Supernova SN 1987a and the Secret Interactions of Neutrinos*, *Phys. Rev. D* **36** (1987) 2895.
- [18] N. D. H. DASS, D. INDUMATHI, A. S. JOSHIPURA and M. V. N. MURTHY, *On the neutrinos from sn 1987a*, *Current Science* **56** (1987) 575.
- [19] A. Mirizzi, I. Tamborra, H.-T. Janka, N. Saviano, K. Scholberg, R. Bollig et al., *Supernova Neutrinos: Production, Oscillations and Detection*, *Riv. Nuovo Cim.* **39** (2016) 1 [1508.00785].
- [20] S. Horiuchi and J. P. Kneller, *What can be learned from a future supernova neutrino detection?*, *J. Phys. G* **45** (2018) 043002 [1709.01515].
- [21] K. Scholberg, *Supernova Neutrino Detection*, *Ann. Rev. Nucl. Part. Sci.* **62** (2012) 81 [1205.6003].
- [22] SUPER-KAMIOKANDE collaboration, M. Ikeda et al., *Search for Supernova Neutrino Bursts at Super-Kamiokande*, *Astrophys. J.* **669** (2007) 519 [0706.2283].
- [23] M. Aglietta et al., *The Most powerful scintillator supernovae detector: LVD*, *Nuovo Cim. A* **105** (1992) 1793.
- [24] N. Y. Agafonova et al., *On-line recognition of supernova neutrino bursts in the LVD detector*, *Astropart. Phys.* **28** (2008) 516 [0710.0259].
- [25] C. A. Duba et al., *HALO: The helium and lead observatory for supernova neutrinos*, *J. Phys. Conf. Ser.* **136** (2008) 042077.
- [26] F. Halzen, J. E. Jacobsen and E. Zas, *Ultrasensitive Antarctic ice as a supernova detector*, *Phys. Rev. D* **53** (1996) 7359 [astro-ph/9512080].
- [27] ICECUBE collaboration, R. Abbasi et al., *IceCube Sensitivity for Low-Energy Neutrinos from Nearby Supernovae*, *Astron. Astrophys.* **535** (2011) A109 [1108.0171].
- [28] DUNE collaboration, B. Abi et al., *Deep Underground Neutrino Experiment (DUNE), Far Detector Technical Design Report, Volume I Introduction to DUNE*, *JINST* **15** (2020) T08008 [2002.02967].
- [29] DUNE collaboration, B. Abi et al., *Deep Underground Neutrino Experiment (DUNE), Far Detector Technical Design Report, Volume II: DUNE Physics*, 2002.03005.
- [30] JUNO collaboration, F. An et al., *Neutrino Physics with JUNO*, *J. Phys. G* **43** (2016) 030401 [1507.05613].
- [31] JUNO collaboration, Z. Djurcic et al., *JUNO Conceptual Design Report*, 1508.07166.
- [32] JUNO collaboration, A. Abusleme et al., *JUNO Physics and Detector*, 2104.02565.

- [33] THEIA collaboration, M. Askins et al., *THEIA: an advanced optical neutrino detector*, *Eur. Phys. J. C* **80** (2020) 416 [[1911.03501](#)].
- [34] K. Abe et al., *Letter of Intent: The Hyper-Kamiokande Experiment — Detector Design and Physics Potential* —, [1109.3262](#).
- [35] N. Jelley, A. B. McDonald and R. G. H. Robertson, *The Sudbury Neutrino Observatory*, *Ann. Rev. Nucl. Part. Sci.* **59** (2009) 431.
- [36] D. A. Roberts, F. D. Becchetti, K. Ashktorab, D. Stewart, J. Janecke, H. R. Gustafson et al., *Deuterated liquid scintillator (ne230) as a fast neutron detector for cold-fusion and other research*, *IEEE Transactions on Nuclear Science* **39** (1992) 532.
- [37] B. W. Sargent, D. V. Booker, P. E. Cavanagh, H. G. Hereward and N. J. Niemi, *The diffusion length of thermal neutrons in heavy water*, *Canadian Journal of Research* **25a** (1947) 134 [<https://doi.org/10.1139/cjr47a-015>].
- [38] J. Dejuren and H. Rosenwasser, *Diffusion length of thermal neutrons in water*, *Journal of Research of the National Bureau of Standards* **51** (1953) 203.
- [39] PARTICLE DATA GROUP collaboration, P. Zyla et al., *Review of Particle Physics*, *PTEP* **2020** (2020) 083C01.
- [40] J. F. Beacom, W. M. Farr and P. Vogel, *Detection of Supernova Neutrinos by Neutrino Proton Elastic Scattering*, *Phys. Rev. D* **66** (2002) 033001 [[hep-ph/0205220](#)].
- [41] B. Dasgupta and J. F. Beacom, *Reconstruction of supernova  $\nu_\mu$ ,  $\nu_\tau$ , anti- $\nu_\mu$ , and anti- $\nu_\tau$  neutrino spectra at scintillator detectors*, *Phys. Rev. D* **83** (2011) 113006 [[1103.2768](#)].
- [42] M. Fukugita, Y. Kohyama and K. Kubodera, *NEUTRINO REACTION CROSS-SECTIONS ON C-12 TARGET*, *Phys. Lett. B* **212** (1988) 139.
- [43] A. Friedland and S. W. Li, *Understanding the energy resolution of liquid argon neutrino detectors*, *Phys. Rev. D* **99** (2019) 036009 [[1811.06159](#)].
- [44] R. Laha and J. F. Beacom, *Gadolinium in water Cherenkov detectors improves detection of supernova  $\nu_e$* , *Phys. Rev. D* **89** (2014) 063007 [[1311.6407](#)].
- [45] R. Laha, J. F. Beacom and S. K. Agarwalla, *New Power to Measure Supernova  $\nu_e$  with Large Liquid Scintillator Detectors*, [1412.8425](#).
- [46] A. Nikrant, R. Laha and S. Horiuchi, *Robust measurement of supernova  $\nu_e$  spectra with future neutrino detectors*, *Phys. Rev. D* **97** (2018) 023019 [[1711.00008](#)].
- [47] M. Kachelriess, R. Tomas, R. Buras, H. T. Janka, A. Marek and M. Rampp, *Exploiting the neutronization burst of a galactic supernova*, *Phys. Rev. D* **71** (2005) 063003 [[astro-ph/0412082](#)].
- [48] S. Nakamura, T. Sato, V. P. Gudkov and K. Kubodera, *Neutrino reactions on deuteron*, *Phys. Rev. C* **63** (2001) 034617 [[nucl-th/0009012](#)].
- [49] J.-W. Chen, G. Rupak and M. J. Savage, *Nucleon-nucleon effective field theory without pions*, *Nucl. Phys. A* **653** (1999) 386 [[nucl-th/9902056](#)].
- [50] M. Butler, J.-W. Chen and X. Kong, *Neutrino deuteron scattering in effective field theory at next-to-next-to-leading order*, *Phys. Rev. C* **63** (2001) 035501 [[nucl-th/0008032](#)].

- [51] S. A. Colgate and R. H. White, *The Hydrodynamic Behavior of Supernovae Explosions*, *Astrophys. J.* **143** (1966) 626.
- [52] H. T. Janka, T. Melson and A. Summa, *Physics of Core-Collapse Supernovae in Three Dimensions: a Sneak Preview*, *Ann. Rev. Nucl. Part. Sci.* **66** (2016) 341 [[1602.05576](#)].
- [53] M. T. Keil, G. G. Raffelt and H.-T. Janka, *Monte Carlo study of supernova neutrino spectra formation*, *Astrophys. J.* **590** (2003) 971 [[astro-ph/0208035](#)].
- [54] E. K. Akhmedov, C. Lunardini and A. Y. Smirnov, *Supernova neutrinos: Difference of muon-neutrino - tau-neutrino fluxes and conversion effects*, *Nucl. Phys. B* **643** (2002) 339 [[hep-ph/0204091](#)].
- [55] A. S. Dighe and A. Y. Smirnov, *Identifying the neutrino mass spectrum from the neutrino burst from a supernova*, *Phys. Rev. D* **62** (2000) 033007 [[hep-ph/9907423](#)].
- [56] J. T. Pantaleone, *Neutrino oscillations at high densities*, *Phys. Lett. B* **287** (1992) 128.
- [57] S. Pastor, G. G. Raffelt and D. V. Semikoz, *Physics of synchronized neutrino oscillations caused by selfinteractions*, *Phys. Rev. D* **65** (2002) 053011 [[hep-ph/0109035](#)].
- [58] H. Duan, G. M. Fuller and Y.-Z. Qian, *Collective neutrino flavor transformation in supernovae*, *Phys. Rev. D* **74** (2006) 123004 [[astro-ph/0511275](#)].
- [59] R. F. Sawyer, *Neutrino cloud instabilities just above the neutrino sphere of a supernova*, *Phys. Rev. Lett.* **116** (2016) 081101 [[1509.03323](#)].
- [60] H. Duan, G. M. Fuller, J. Carlson and Y.-Z. Qian, *Simulation of Coherent Non-Linear Neutrino Flavor Transformation in the Supernova Environment. 1. Correlated Neutrino Trajectories*, *Phys. Rev. D* **74** (2006) 105014 [[astro-ph/0606616](#)].
- [61] G. L. Fogli, E. Lisi, A. Marrone and A. Mirizzi, *Collective neutrino flavor transitions in supernovae and the role of trajectory averaging*, *JCAP* **12** (2007) 010 [[0707.1998](#)].
- [62] B. Dasgupta, A. Dighe, G. G. Raffelt and A. Y. Smirnov, *Multiple Spectral Splits of Supernova Neutrinos*, *Phys. Rev. Lett.* **103** (2009) 051105 [[0904.3542](#)].
- [63] S. Bhattacharyya and B. Dasgupta, *Fast Flavor Depolarization of Supernova Neutrinos*, *Phys. Rev. Lett.* **126** (2021) 061302 [[2009.03337](#)].
- [64] L. Johns, H. Nagakura, G. M. Fuller and A. Burrows, *Neutrino oscillations in supernovae: angular moments and fast instabilities*, *Phys. Rev. D* **101** (2020) 043009 [[1910.05682](#)].
- [65] G. Dutta, D. Indumathi, M. V. N. Murthy and G. Rajasekaran, *Neutrinos from stellar collapse: Comparison of signatures in water and heavy water detectors*, *Phys. Rev. D* **64** (2001) 073011 [[hep-ph/0101093](#)].
- [66] W. Schadow and W. Sandhas, *Radiative capture of protons by deuterons*, *Phys. Rev. C* **59** (1999) 607 [[nucl-th/9808048](#)].
- [67] J.-S. Lu, Y.-F. Li and S. Zhou, *Getting the most from the detection of Galactic supernova neutrinos in future large liquid-scintillator detectors*, *Phys. Rev. D* **94** (2016) 023006 [[1605.07803](#)].

- [68] H.-L. Li, Y.-F. Li, M. Wang, L.-J. Wen and S. Zhou, *Towards a complete reconstruction of supernova neutrino spectra in future large liquid-scintillator detectors*, *Phys. Rev. D* **97** (2018) 063014 [[1712.06985](#)].
- [69] H.-L. Li, X. Huang, Y.-F. Li, L.-J. Wen and S. Zhou, *Model-independent approach to the reconstruction of multiflavor supernova neutrino energy spectra*, *Phys. Rev. D* **99** (2019) 123009 [[1903.04781](#)].
- [70] H. Nagakura, *Retrieval of energy spectra for all flavours of neutrinos from core-collapse supernova with multiple detectors*, *Mon. Not. Roy. Astron. Soc.* **500** (2020) 319 [[2008.10082](#)].
- [71] J. Ziegler, J. Biersack and M. Ziegler, *SRIM, the Stopping and Range of Ions in Matter*. SRIM Company, 2008.
- [72] J. B. Birks, *Scintillations from organic crystals: Specific fluorescence and relative response to different radiations*, *Proceedings of the Physical Society. Section A* **64** (1951) 874.
- [73] W. J. Marciano and Z. Parsa, *Neutrino electron scattering theory*, *J. Phys. G* **29** (2003) 2629 [[hep-ph/0403168](#)].
- [74] R. C. Malone et al., *Neutron-neutron quasifree scattering in neutron-deuteron breakup at 10 MeV*, *Phys. Rev. C* **101** (2020) 034002 [[2003.14396](#)].
- [75] A. V. Lyashenko et al., *Performance of Large Area Picosecond Photo-Detectors (LAPPD<sup>TM</sup>)*, *Nucl. Instrum. Meth. A* **958** (2020) 162834 [[1909.10399](#)].
- [76] F. Capozzi, B. Dasgupta and A. Mirizzi, *Model-independent diagnostic of self-induced spectral equalization versus ordinary matter effects in supernova neutrinos*, *Phys. Rev. D* **98** (2018) 063013 [[1807.00840](#)].
- [77] SUPER-KAMIOKANDE collaboration, H. Zhang et al., *Supernova Relic Neutrino Search with Neutron Tagging at Super-Kamiokande-IV*, *Astropart. Phys.* **60** (2015) 41 [[1311.3738](#)].
- [78] B. Chauhan, B. Dasgupta, V. Datar, M. Diwan, D. Indumathi and M. V. N. Murthy, *White Paper*, in preparation.
- [79] SUPER-KAMIOKANDE collaboration, K. Abe et al., *Search for proton decay via  $p \rightarrow e^+\pi^0$  and  $p \rightarrow \mu^+\pi^0$  in 0.31 megaton-years exposure of the Super-Kamiokande water Cherenkov detector*, *Phys. Rev. D* **95** (2017) 012004 [[1610.03597](#)].
- [80] KAMLAND collaboration, K. Asakura et al., *Search for the proton decay mode  $p \rightarrow \bar{\nu}K^+$  with KamLAND*, *Phys. Rev. D* **92** (2015) 052006 [[1505.03612](#)].
- [81] SNO collaboration, S. N. Ahmed et al., *Constraints on nucleon decay via 'invisible' modes from the Sudbury Neutrino Observatory*, *Phys. Rev. Lett.* **92** (2004) 102004 [[hep-ex/0310030](#)].
- [82] H. Murayama and C. Pena-Garay, *Neutrinoless double beta decay in light of SNO salt data*, *Phys. Rev. D* **69** (2004) 031301 [[hep-ph/0309114](#)].
- [83] SNO+ collaboration, J. Paton, *Neutrinoless Double Beta Decay in the SNO+ Experiment*, in *Prospects in Neutrino Physics*, 3, 2019, [1904.01418](#).

- [84] A. Bhusal, N. Houston and T. Li, *Searching for Solar Axions Using Data from the Sudbury Neutrino Observatory*, *Phys. Rev. Lett.* **126** (2021) 091601 [[2004.02733](#)].
- [85] C. Lujan-Peschard, G. Pagliaroli and F. Vissani, *Spectrum of Supernova Neutrinos in Ultra-pure Scintillators*, *JCAP* **07** (2014) 051 [[1402.6953](#)].
- [86] A. Gallo Rosso, F. Vissani and M. C. Volpe, *What can we learn on supernova neutrino spectra with water Cherenkov detectors?*, *JCAP* **04** (2018) 040 [[1712.05584](#)].
- [87] S. W. Li, L. F. Roberts and J. F. Beacom, *Exciting Prospects for Detecting Late-Time Neutrinos from Core-Collapse Supernovae*, *Phys. Rev. D* **103** (2021) 023016 [[2008.04340](#)].